Feedback amplification loop drives malignant growth in epithelial tissues

Mariana Muzzopappa[a], Lada Murcia[a], and Marco Milán[a,b,1]

[a]Institute for Research in Biomedicine (IRB Barcelona), The Barcelona Institute of Science and Technology, 08028 Barcelona, Spain; and [b]Institució Catalana de Recerca i Estudis Avançats (ICREA), 08010 Barcelona, Spain

Edited by Norbert Perrimon, Harvard Medical School, Boston, MA, and approved July 25, 2017 (received for review February 1, 2017)

Interactions between cells bearing oncogenic mutations and the surrounding microenvironment, and cooperation between clonally distinct cell populations, can contribute to the growth and malignancy of epithelial tumors. The genetic techniques available in *Drosophila* have contributed to identify important roles of the TNF-α ligand Eiger and mitogenic molecules in mediating these interactions during the early steps of tumor formation. Here we unravel the existence of a tumor-intrinsic—and microenvironment-independent—self-reinforcement mechanism that drives tumor initiation and growth in an Eiger-independent manner. This mechanism relies on cell interactions between two functionally distinct cell populations, and we present evidence that these cell populations are not necessarily genetically different. Tumor-specific and cell-autonomous activation of the tumorigenic JNK stress-activated pathway drives the expression of secreted signaling molecules and growth factors to delaminating cells, which nonautonomously promote proliferative growth of the partially transformed epithelial tissue. We present evidence that cross-feeding interactions between delaminating and nondelaminating cells increase each other's sizes and that these interactions can explain the unlimited growth potential of these tumors. Our results will open avenues toward our molecular understanding of those social cell interactions with a relevant function in tumor initiation in humans.

tumor microenvironment | chromosomal instability | epithelial tumor | Wingless | JNK

Cancer development is a multistep process that involves altered cellular signaling, resulting in limitless replicative potential of the cells, evasion of apoptosis, tissue invasion, and metastasis (1). Carcinomas, tumors of epithelial origin, are often associated with inflammatory cells and activated fibroblasts, the tumor microenvironment (TME), which plays a critical role in cancer progression and in the colonization of target tissues (reviewed in ref. 2). These tumors are genetically heterogeneous, and intratumor cooperation between different subclonal cell populations can also contribute to the growth of these tumors (reviewed in ref. 3).

In recent decades, *Drosophila* models of epithelial tumors have been shown to reproduce key aspects of cancer development and have become useful model systems to characterize the cellular and molecular determinants that initiate tumorigenesis (reviewed in ref. 4). The epithelial primordia of the adult ectoderm, the so-called imaginal discs, provide the advantage that individual cells can be tracked, and the tissue can be manipulated genetically in temporal and spatial manner. In malignant neoplastic tumors of epithelial origin, activation of the c-Jun N-terminal kinase (JNK) stress cascade plays a tumor-suppressing or a tumor-promoting role depending on the activity of the apoptotic pathway (5–7). In neoplastic tumors resulting from mutations in the tumor suppressor genes *scribbled* (*scrib*) or *discs large 1* (*dlg1*), encoding for cell polarity determinants, JNK activates the apoptotic program and induces the removal of transformed cells from the tissue, thus limiting tumor growth (6–8). By contrast, in those tumors in which the apoptotic pathway is being inhibited, thus mimicking an important hallmark of human cancer (1), sustained activation of JNK becomes tumor-promoting. Activation of a JNK-dependent transcriptional program in these tumors induces the expression of a collection of well-defined target genes that contribute to driving unlimited growth, malignancy, and metastatic behavior (8–12). The genetic techniques available in *Drosophila* have unraveled how interactions between clones of cells bearing oncogenic mutations and the surrounding WT epithelium contribute to JNK activation, tumor growth, and malignancy, and have identified a major role of the TNF-α ligand Eiger and its receptor Grindelwald (Grnd) in mediating these interactions (13–16). Moreover, intratumor cooperation between clonally distinct cell populations can also contribute to the growth of these tumors (17).

Epithelial tumors generated in larval primordia are embedded in the open circulatory system of the fly and are infiltrated by circulating immune cells [hemocytes (5, 18)] and associated with resident mesenchymal cells [myoblasts (19)]. These two cell populations are also part of the TME and are amplified by cell proliferation as a response to the expression of mitogenic molecules produced by tumor cells (18, 19). In tumors resulting from mutations in *scrib* or *dlg1*, attached hemocytes restrict growth by limiting basement membrane disruption (18) and enhancing JNK-mediated removal of transformed cells by apoptosis (5). By contrast, proliferating myoblasts promote epithelial transformation in tumors resulting from the oncogenic cooperation between the EGF receptor and loss of epigenetic factors (19).

Here we have used two well-defined JNK-driven *Drosophila* neoplastic tumor models of epithelial origin to address the relative contribution of TME-independent and tumor-intrinsic mechanisms to the unlimited growth potential of these tumors. We used the *GAL4/UAS* system to drive tumorigenesis in large

Significance

Progression of epithelial tumors and successful colonization of target tissues rely in many cases on the presence of the tumor microenvironment (TME), which acts as a niche to provide secreted signaling molecules and growth factors to tumor cells. Here we used *Drosophila* to show that the TME is not an absolute requirement for the growth of epithelial tumors caused by chromosomal instability (CIN) or compromised cell polarity. Instead, tumor growth is driven by a feedback amplification loop between two well-defined—but not necessarily genetically different—tumor cell populations. As CIN or impaired cell polarity are frequently observed in human tumors of epithelial origin, our results will provide insight to the mechanistic understanding of their unlimited growth potential.

Author contributions: M. Muzzopappa and M. Milán designed research; M. Muzzopappa and L.M. performed research; M. Muzzopappa, L.M., and M. Milán analyzed data; and M. Milán wrote the paper.

The authors declare no conflict of interest.

This article is a PNAS Direct Submission.

[1]To whom correspondence should be addressed. Email: marco.milan@irbbarcelona.org.

This article contains supporting information online at www.pnas.org/lookup/suppl/doi:10.1073/pnas.1701791114/-/DCSupplemental.

territories, thus reducing interactions with surrounding WT epithelial cells and generating genetically homogenous tumor-like structures. We combined allograft transplantations and two independent transactivation systems to demonstrate that JNK activation and tumor initiation in these models are largely unaffected by the genetic ablation of circulating immune cells and resident mesenchymal cells. Our data also indicate that JNK activation and tumor growth do not depend on the activity of Eiger, the *Drosophila* TNF-α (20, 21), and its receptor Grnd (14). We unravel the use of cell-autonomous and tumor-specific molecular mechanisms to activate a common JNK kinase (JNKK)/JNK core signaling pathway that induces a shared transcriptional program to initiate tumorigenesis. Our results support the proposal that intratumor social interactions between functionally distinct cell populations can drive unlimited growth in the absence of the TME. Remarkably, these two cell populations are not necessarily genetically different, as opposed to the cooperation between clonally distinct cell populations reported in vertebrate and invertebrate tumor models (3, 4). We propose that the previously reported roles of the TME and Eiger in tumorigenesis are mainly restricted to mediating interactions between tumor-initiating and surrounding WT epithelial cells (13–16).

Results

Two Molecularly Distinct Tumor Models, Three Cell Populations, and Eiger Expression. We selected two different epithelial tumor models that rely on the activation of JNK and the transcriptional induction of a common set of target genes responsible for their high mitotic activity and metastatic behavior and for causing malignancy to the host. The first model, the chromosomal instability (CIN) model, is based on the protumorigenic action of CIN, a high rate of gain or loss of whole chromosomes or parts of them (22). Depletion of the spindle assembly checkpoint (SAC) by means of GAL4-mediated expression of RNAi forms of the SAC genes *bub3* or *rod* causes chromosome segregation errors, and the resulting aneuploid cells, cells with extra or missing chromosomes, delaminate from the tissue and activate the JNK transcriptional program that induces apoptosis (23). Blockade of the apoptotic program by expressing the baculovirus protein P35, which binds and inhibits the activity of effector caspases Dcp1 and DrIce (24), leads to activation of JNK in aneuploid cells and to the robust transcriptional induction of JNK-regulated target genes with a role in driving tumorigenesis (25). Ectopic expression of mitogenic molecules, such as Wingless (Wg) and IL-6–like Upd cytokines, contributes to tumor growth, whereas ectopic expression of matrix metalloproteinases (MMPs; Fig. 1*B*) results in basement membrane degradation. The second model system, the polarity-impaired model, is based on the conserved oncogenic cooperation between the activated form of Ras (Ras-V12) and the loss of polarity determinants *scrib* and *dlg1* (7, 26–29). Whereas GAL4-mediated expression of Ras-V12 induces hyperplastic growth by increasing the expression of the growth-promoting proto-oncogene dMyc and driving G1-S transition (30), reduction in the expression levels of *scrib* or *dlg1* by the use of mutant alleles or RNAi forms leads to neoplasia, JNK activation, and, again, robust transcriptional induction of JNK-regulated genes with a role in driving tumorigenesis, such as Wg, Upd cytokines, and MMPs (Fig. 1*B*) (7, 12, 26). The growth potential of these two tumor models can be easily quantified and visualized in allograft experiments in

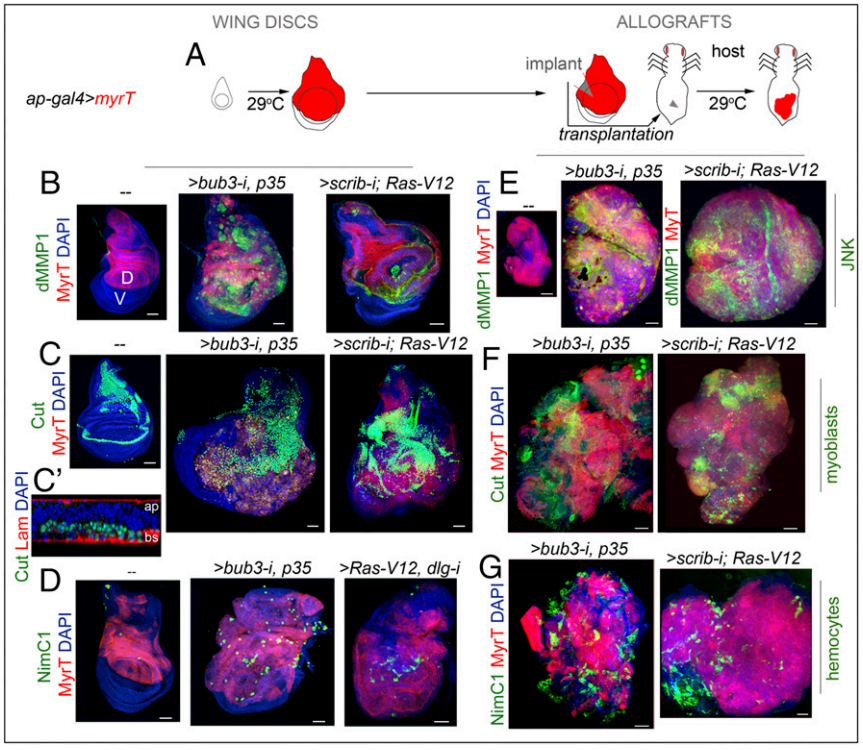

Fig. 1. *Drosophila* JNK-dependent epithelial tumor models, hemocyte recruitment, and myoblast proliferation. (*A*) Cartoon showing the expression of tumor-inducing transgenes in the dorsal (marked as "D") compartment (red) of larval wing discs (*Left*) and allograft transplantations into the abdomen of female hosts (*Right*). Fly hosts were maintained at 29 °C. (*B–G*) Larval wing primordia (*B–D*) and allograft transplants (*E–G*) expressing the indicated transgenes in the dorsal compartment under the control of the *ap-GAL4* driver and stained with DAPI (blue), MyrT (red), dMMP1 (green, *B* and *E*), Cut (green, *C*, *C′*, and *F*), NimC1 (green, *D* and *G*), and laminin (Lam; red, *C′*). In *C′*, cross-section of the proximal part of the wing disk is shown to visualize the localization of the myoblasts underneath the main epithelium. Apical (ap) and basal (bs) sides of the epithelium are marked. Transplants were extracted 5 days (*scrib-i*; *Ras-V12*) or 12 days (*bub3-i*, *p35*) after implantation. (Scale bars, 50 μm.)

which a small piece of the tumor (i.e., implant) is able to regenerate a solid tumor in the abdomen of female adult hosts several days after implantation (Fig. 1 *A* and *E*). In these allografts, the growth capacity of WT tissues is shown to be limited, and JNK is not induced (Fig. 1*E*). Remarkably, CIN and polarity-impaired tumors induce the amplification of the resident myoblast population, which can be marked by the expression of Cut (Fig. 1 *C* and *F*) (31) or Twist (Fig. S1) transcription factors. These two models also share a strong capacity to attract circulating hemocytes, labeled by the expression of Nimrod C1 [NimC1; a phagocytosis receptor used as a marker of the most abundant type of hemocytes, the plasmatocytes (32); Fig. 1 *D* and *G*]. Progression to neoplasia in CIN and polarity-impaired tumors rely on the activation of JNK and on a collection of transcription factors that induce a tumorigenic transcriptional program (10). Eiger, the unique member of the TNF superfamily of ligands in *Drosophila* (20, 21), activates the JNK signaling pathway by binding to the TNF-α receptor Grnd (14), and has been proposed to play a tumor-promoting role in the presence of Ras-V12 (5). Interestingly, expression of Eiger, visualized by the use of two different reporter constructs and an antibody (*Materials and Methods*), was observed in the myoblast population of WT and CIN and polarity-impaired wing primordia (Fig. 2 *A*–*C* and Fig. S1), and became ectopically expressed in tumor epithelial cells [labeled by the expression of myristoylated Tomato (MyrT); Fig. 2 *D* and *F* and Fig. S1] as well in those hemocytes attached to the tumor [Fig. 2 *E* and *G*, labeled by the expression of the hemocyte-specific transmembrane protein Hemese (He)] (33). We observed that Eiger expression was also induced in hemocytes from the host that were attached to the allografted tumors (Fig. 2*H*). Based on these observations, the potential role of TME cells in tumor initiation and the requirement of Eiger for JNK activation will be analyzed.

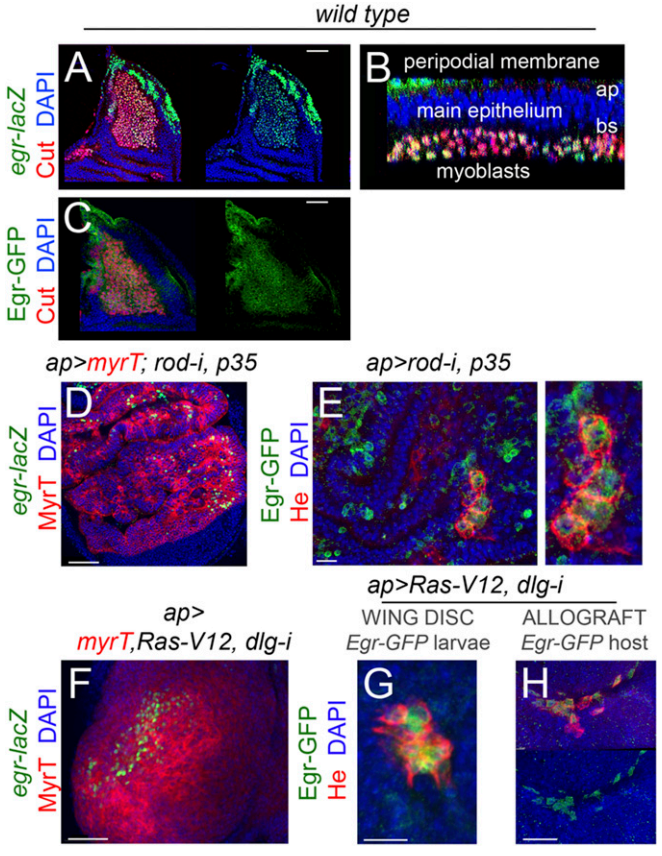

Fig. 2. Eiger expression in development and in JNK-driven epithelial tumors. (*A*–*H*) Larval wing primordia from WT individuals (*A*–*C*) or from individuals expressing the indicated transgenes under the control of the *ap-GAL4* driver (*D*–*H*) and stained for DAPI (blue, *A*–*H*), Cut (red in *A*–*C*), *eiger-lacZ* (green, *A*, *B*, *D*, and *F*), Eiger-GFP (green, *C*, *E*, *G*, and *H*), He (red, *E*, *G*, and *H*), and MyrT (red, *D* and *F*). Eiger is expressed in myoblasts (labeled by the expression of Cut) in WT wing discs (*A*–*C*) and becomes activated in a scattered pattern in epithelial cells (labeled by the expression of MyrT) and recruited hemocytes (labeled by the expression He) in JNK-driven tumor-like overgrowths (*D*–*H*). (Scale bars, *A*, *C*, *D*, *F*, and *H*, 50 μm; *E* and *G*, 15 μm.)

JNK Activation and Tumor Growth in the Absence of Hemocytes. We first analyzed the contribution of hemocytes to tumor initiation. For this purpose, we performed allograft transplantations into the abdomen of adult females and analyzed JNK activation and growth of these allografts upon genetic ablation of adult hemocytes. Females carrying the hemocyte-specific *hemese-GAL4* (*he-GAL4*) driver, the *tub-GAL80ts* transgene, and the *UAS-GFP* and *UAS-reaper* constructs were used as hosts. The temperature-sensitive GAL80 (GAL80ts) molecule, which represses GAL4 transcriptional activity at low temperatures (18 °C) (34), was used to control expression of the proapoptotic gene *reaper* by shifting the animals from 18 °C to 29 °C a few hours before allograft transplantation. Adult females carrying the *he-GAL4* driver and the *UAS-GFP* transgene were used as controls. We also used the GAL80ts molecule and the temperature shifts to initiate transgene expression and tumorigenesis in larval tissues when they had been transplanted into the adult abdomen. As a proof of concept, larval wing primordia raised at 18 °C and containing the *ap-GAL4* driver and the *tub-GAL80ts* and the corresponding *UAS* transgenes showed no overgrowth phenotype and no obvious effect on JNK activation, as monitored by the expression of the JNK target *Drosophila* matrix metalloproteinase 1 (dMMP1) (Fig. 3*A*; note the endogenous and JNK-independent expression of dMMP1 in the trachea marked by arrows). Very few hemocytes, if any, were observed in these wing discs (Fig. 3*A*, arrowheads). As depicted in Fig. 3*B*, a small piece of these wing discs was transplanted into the abdomen of adult hosts that were then maintained at 29 °C to initiate transgene expression. Note that the implanted piece consists mainly of cells expressing the tumor-initiating transgenes. The implanted tissues were dissected and processed for immunofluorescence after a period of 5 or 12 days for the CIN and polarity-impaired tumor models, respectively. Initiation of transgene expression in the transplanted tissues drove tumor growth (Fig. 3 *C* and *G*), induced a 1,000-fold increase in tissue size (Fig. 3*M*), and activated JNK, as monitored by the expression of dMMP1 (Fig. 3 *D′* and *H′*). Interestingly, these tumors recruited a large number of circulating hemocytes of the adult host, labeled by the expression of GFP (Fig. 3 *D* and *H*) or by the expression of NimC1 (Fig. 3 *I* and *I′*). Recruited hemocytes expressed Eiger (Fig. 2*H*), engulfed cell debris coming from the tumor (labeled by MyrT; Fig. S2), and deposited collagen IV (labeled by the Viking-GFP fusion protein), a fundamental element of epithelial basement membranes (Fig. S2). When the hemocyte cell population was ablated by the expression of *reaper* (Fig. 3 *E*, *F*, and *J*–*L*), initiation of transgene expression in the transplanted tissues was also able to drive tumor growth (Fig. 3 *E*, *F*, *J*, and *K*) and JNK activation (Fig. 3 *F′* and *K′*). Surprisingly, JNK activation and tumor size were both unaffected by the absence of hemocytes (quantified in Fig. 3*M*), but the amount of collagen IV deposited in the tumor was clearly reduced (Fig. S2). Altogether, our results indicate, as previously shown (18), that hemocytes deposit collagen IV in the tumor, most probably to reconstitute the basement membrane, and they engulf cellular debris. However, our data indicate that these hemocytes are not an absolute requirement for tumor initiation and JNK activation in CIN and polarity-impaired tumor models.

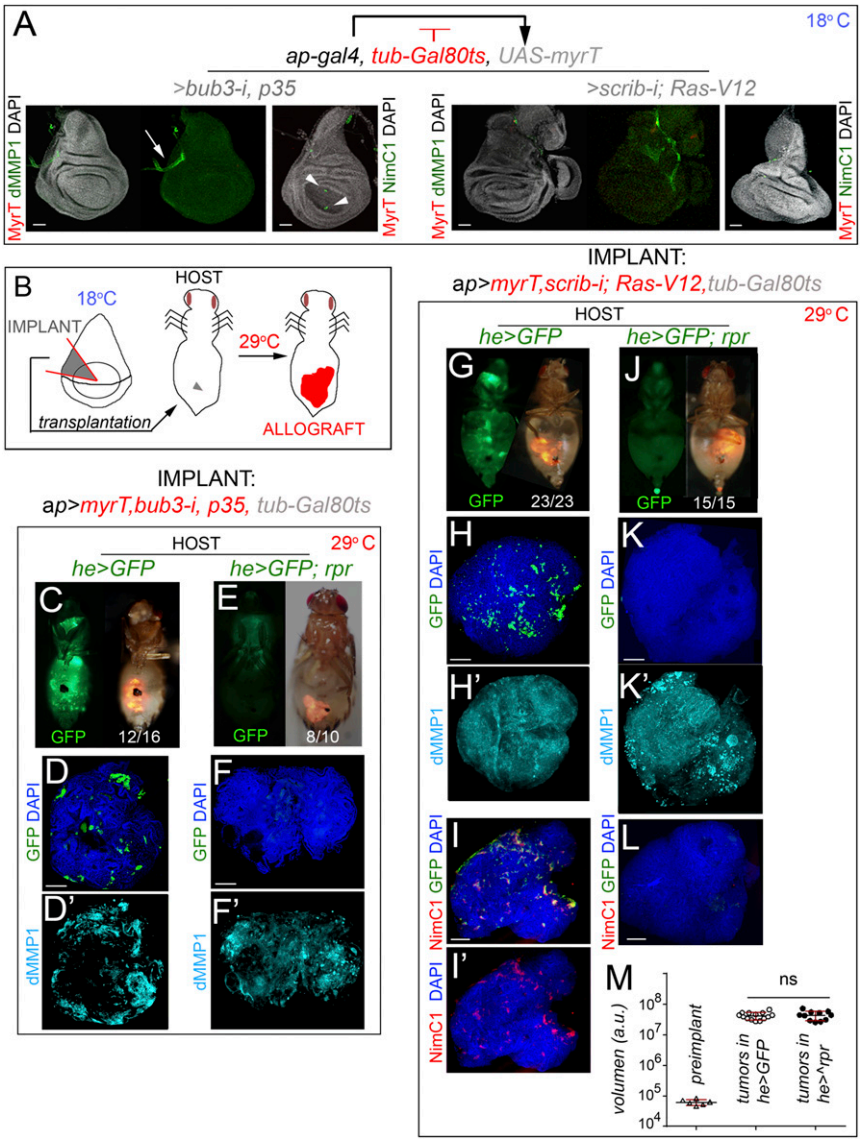

Fig. 3. JNK activation and tumor-like growth in the absence of hemocytes. (*A*) Larval wing primordia of the indicated genotypes, raised at 18 °C to turn off transgene expression in a GAL80-dependent manner, and stained for DAPI (gray), MyrT (red), and dMMP1 (green) or NimC1 (green, *Right*). (Scale bars, 50 μm.) MyrT is not expressed and dMMP1 is not induced under these circumstances. Arrow points to the endogenous expression of dMMP1 in the trachea and arrowheads point to a few hemocytes recruited to control wing primordia. (*B*) Cartoon showing the allograft-transplantation protocol. Wing primordia carrying CIN or *scrib-i*; *Ras-V12* transgenes under control of the *ap-GAL4* driver, and silenced with the GAL80ts factor, were dissected from L3 larvae raised at 18 °C, cut into small pieces, and injected into the abdomen of young adult females. Fly hosts were then transferred to a temperature of 29 °C to induce transgene expression. (*C*, *E*, *G*, and *J*) Micrographs of adult flies carrying MyrT-labeled (red) implants of the indicated genotypes and expressing GFP (green) under the *he-GAL4* driver. Host flies were maintained at 29 °C to induce transgene expression; images were taken 5 days (*G* and *I*) or 12 days (*C* and *E*) after implantation; ratios indicating the reproducibility of the phenotype are shown. In *E* and *J*, host flies expressed the proapoptotic gene *reaper* under the control of the *he-GAL4* driver. (*D*, *D*′, *F*, *F*′, and *H*–*L*) Allograft transplants of the indicated genotypes stained to visualize GFP (green, *D*, *F*, *H*, *I*, and *K*) or NimC1 (red, *I*, *I*′, and *L*), dMMP1 (cyan, *D*′, *F*′, *H*′, *K*′), and DAPI (green, *D*, *F*, *H*, *I*, *I*′, *K*, and *L*). Transplants were extracted 5 days (*H*–*L*) or 12 days (*D*–*F*′) after implantation. (Scale bars, 100 μm.) (*M*) Histogram plotting the size [in arbitrary units (a.u.)] of preimplanted wing disc pieces (*Left*) or allograft transplants expressing *scrib-i*; *Ras-V12* and implanted in adult flies expressing *GFP* (*Middle*) or *GFP* and *reaper* (*Right*) transgenes. Error bars indicate SD. No statistical difference (ns) in allograft size was observed upon induction of *reaper* expression in the adult hemocytes [$P(0.05) = 0.6007$]. Volume (preimplanted wing disc) = $6.17.10^4 \pm 1.3.10^4$ ($n = 6$). Volume (allograft in *he>GFP* hosts) = $4.18.10^7 \pm 1.13.10^7$ ($n = 14$). Volume (allograft in *he>rpr* hosts) = $4.35.10^7 \pm 1.5.10^7$ ($n = 11$).

JNK Activation and Tumor Growth in the Absence of Myoblasts. Myoblasts play a critical role in EGFR-driven epithelial tumors by providing secreted factors that enhance tumor growth (19). As we observed that this population is also the major source of Eiger expression in CIN and polarity-impaired tumors (Fig. 2), we next addressed the potential contribution of the myoblast population to JNK activation and tumor initiation. The *GAL4*/*UAS* and *lexA*/*lexO* systems were combined to induce tumor formation in epithelial cells and simultaneously ablate the myoblast population by the expression of the proapoptotic gene *reaper*. We used the myoblast-specific *15B03-lexA* driver for this purpose (Fig. 4*G*) (19). Myoblasts were marked in all experiments by the expression of the Twist transcription factor. As expression of *reaper* under the control of the *15B03-lexA* driver was not able to genetically ablate these cells in CIN and polarity-impaired tumors using the *ap-GAL4* driver (Fig. S3 and *SI Results*), we switched to the *hh-GAL4* driver, whose expression is restricted to epithelial cells. In this case, in both WT wing discs and CIN and polarity-impaired tumors,

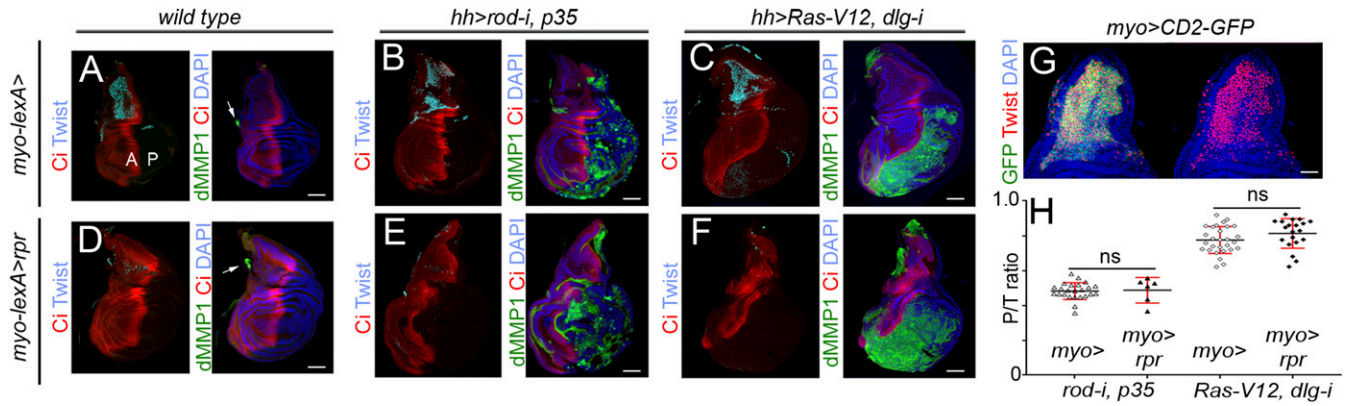

Fig. 4. JNK activation and tumor-like growth upon depletion of the myoblast cell population. (*A–F*) Larval wing primordia of the indicated genotypes stained for Ci (red) and Twist (cyan; *Left*) and DAPI (blue) and dMMP1 (green; *Right*). (*D–F*) Larvae expressed the proapoptotic gene *reaper* under the control of the *15B03-lexA* (*myo-lexA)* driver. Anterior (marked as "A") and posterior (marked as "P") compartments are marked. *hh-GAL4* drives expression to posterior cells, and Ci labels the anterior compartment. Arrows in *A* and *D* point to the endogenous expression of dMMP1 in the trachea of WT primordia. Note in *B*, *C*, *E*, *F* (*Right*) the ectopic expression of dMMP1 in the posterior compartment. Some background staining is observed in the folds of the anterior compartment in some discs (e.g., *E*). (*g*) Notum of a larval wing primordium expressing CD2-GFP (green) under the control of the *myo-lexA* driver and stained for DAPI (blue) and Twist (red). (Scale bars, *A–F*, 50 μm; *G*, 30 μm.) (*h*) Histogram plotting the ratio between the size of the posterior (marked as "P") compartment (labeled by the absence of Ci in *A–F*) and the total size (marked as "T") of wing discs of the indicated genotypes. Error bars indicate SD ($n > 6$ in all cases). No statistical difference (ns) in posterior compartment to total wing primordia (P/T) ratio was observed upon depletion of the myoblast population in the two tumor models [P(*rod-i, p35*) = 0.83, and P(*Ras-V12, dlg1-i*) = 0.1139].

15B03-lexA–driven *reaper* expression was able to deplete the whole myoblast population (Fig. 4 *D–F*). We observed that JNK activation and tumor size were both unaffected by the absence of myoblasts (Fig. 4 *A–F*; quantified in Fig. 4*H*). These results indicate that JNK-driven tumor-like overgrowth in CIN and polarity-impaired tumors is largely independent of the tumor-associated myoblasts. Interestingly, tumor growth and JNK activation were still observed upon simultaneous depletion of the myoblast and hemocyte cell populations (Fig. S2).

JNK Activation and Tumor Growth in the Absence of Eiger. Based on the aforementioned results indicating that TME cells—recruited hemocytes and resident myoblasts—do not have any impact on tumor initiation and JNK activation in CIN and polarity-impaired epithelial tumors, we next addressed the functional role of the ectopic expression of Eiger observed in epithelial cells (Fig. 2 *D–F* and Fig. S1). For this purpose, we depleted Eiger in CIN and polarity-impaired tumors by the use of an RNAi form against *eiger* or by inducing clones of cells homozygous for a null allele of *eiger* (*eiger*^{3}) (21). JNK activation, monitored by the expression of dMMP1, and the resulting tissue overgrowth were both largely unaffected by the coexpression of *eiger-RNAi* together with the tumor-inducing transgenes (Fig. 5 *A*, *B*, *F*, and *G*; quantified in Fig. 5 *C* and *H*). Consistent with these results, JNK activation was still observed in clones of cells mutant for *eiger* and expressing the CIN and polarity-impaired tumor-inducing transgenes (Fig. 5 *D*, *E*, *I*, and *J*). We next induced CIN and polarity-impaired tumors upon removal of Eiger in the whole animal by driving the tumor-inducing transgenes in *eiger*^{1} mutants (*eiger*^{1} is a null allele of *eiger*) (21). Complete loss of Eiger activity did not have any impact on JNK activation or tumor growth (Fig. 6 *A–D*; quantified in Fig. 6*O*). Eiger drives JNK activation in epithelial cells through its recently identified receptor Grnd (14). JNK activation and tumor growth were largely unaffected by targeted depletion of Grnd in epithelial cells with a *grnd-RNAi* form (Fig. 6 *E–H*; quantified in Fig. 6*P*) or by removal of Grnd in the whole animal by the use of a *grnd*^{MI05292} mutant allele (Fig. 6 *I–L*; quantified in Fig. 6*Q*). JNK activation in clones of cells expressing the tumor-inducing transgenes was also still observed upon *grnd* depletion, albeit at lower levels (Fig. 6 *M* and *N*, white arrows). We noticed that the capacity of *grnd* depletion to reduce the levels of JNK activation was stronger in clones of cells expressing the tumor-inducing transgenes in the eye primordia (Fig. S4) (14). The

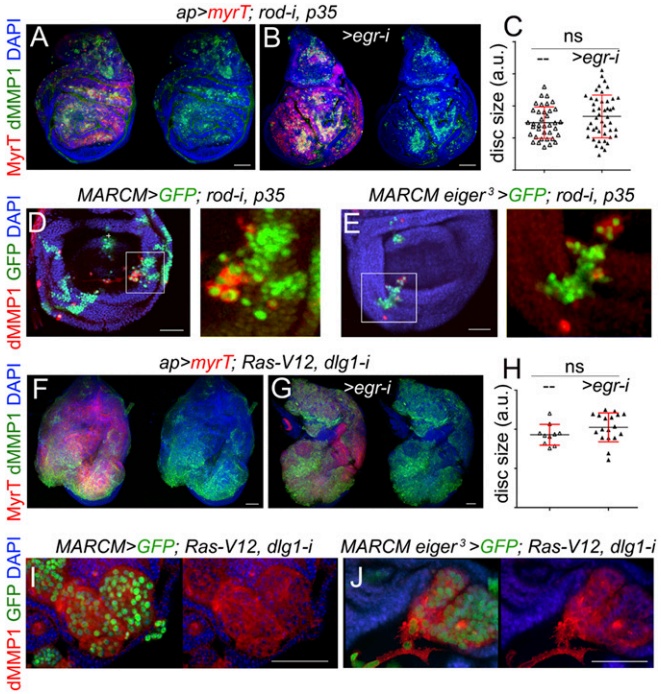

Fig. 5. Eiger is not required in epithelial cells to drive JNK activation and tumor-like growth. (*A*, *B*, *F*, and *G*) Larval wing primordia expressing the indicated transgenes under the control of the *ap-GAL4* driver and stained for DAPI (blue), MyrT (red), and dMMP1 (green). (*D*, *E*, *I*, and *J*) Larval wing primordia with clones of WT (*D* and *I*) or *eiger*^{3} mutant cells (*E* and *J*) induced by the mosaic analysis with a repressible cell marker (MARCM) technique and expressing the indicated transgenes. Clones were positively labeled by the expression of GFP (green), and the tissue was stained for dMMP1 (red) and DAPI (blue). (Scale bars, 50 μm.) (*C* and *H*) Histograms plotting the size [in arbitrary units (a.u.)] of larval wing primordia of the indicated genotypes. Error bars indicate SD ($n > 10$ in all cases). No statistical difference was observed between *eiger-RNAi* expressing and nonexpressing samples [P(*c*) = 0.1425 and P(h) = 0.1659].

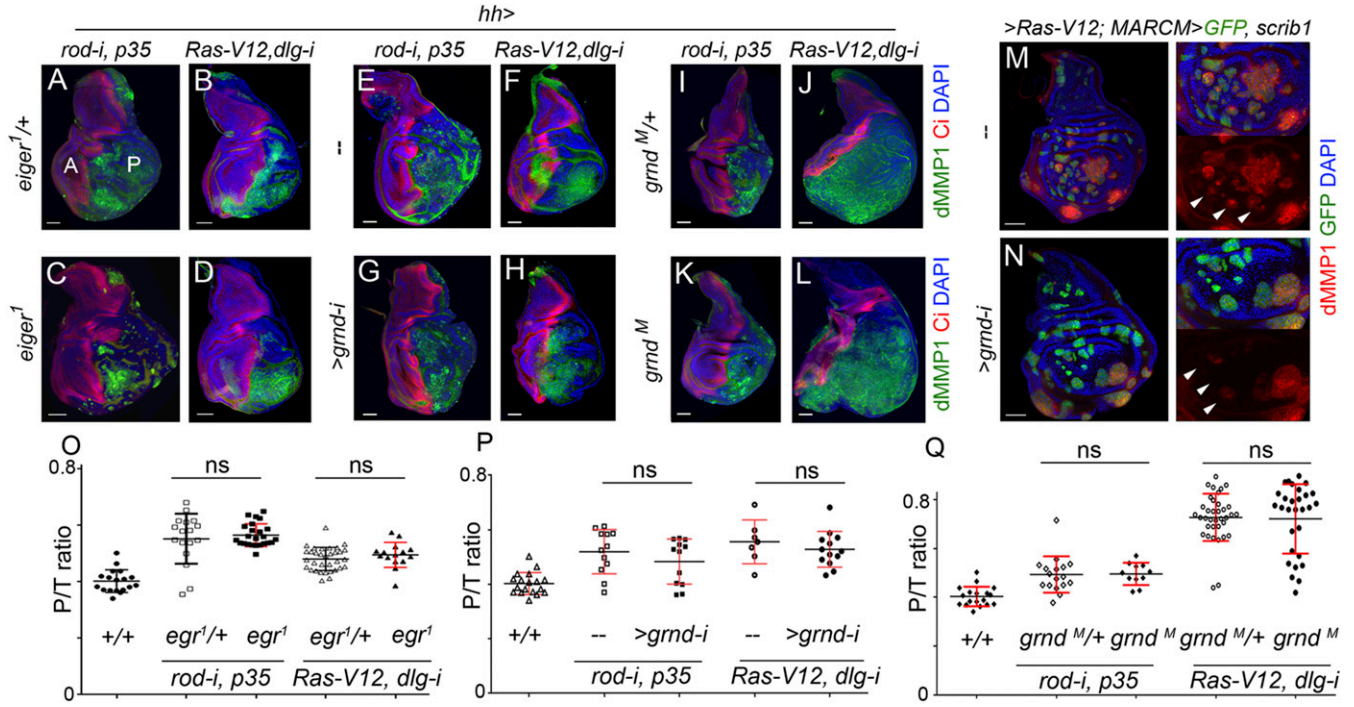

Fig. 6. JNK activation and tumor-like growth in the absence of Eiger and Grnd. (*A*–*L*) Larval wing primordia of the indicated genotypes and stained for DAPI (blue), Ci (red), and dMMP1 (green). *hh-GAL4* drives expression to posterior (marked as "P") cells, and Ci labels the anterior (marked as "A") compartment. In *C*, *D*, *G*, *H*, *K*, and *L*, larvae were homozygous mutant for *eiger* or *grnd* or expressing *grnd-i*. Larvae shown in *A*, *B*, *E*, *F*, *I*, and *J* served as controls. (*M* and *N*) Larval wing primordia with clones of cells induced by the MARCM technique and expressing the indicated transgenes. Clones were positively labeled by the expression of GFP (green), and the tissue was also stained for dMMP1 expression (red) and DAPI (blue). dMMP1 was cell-autonomously induced in WT and *grnd-i*–expressing cells (white arrows), albeit at lower levels in *grnd-i*–expressing cells. (Scale bars, 50 μm.) (*O*–*Q*) Histograms plotting the ratio between the size of the posterior compartment (labeled by the absence of Ci in *A*–*L*) and the total size (marked as "T") of wing discs of the indicated genotypes. Error bars indicate SD ($n > 7$ in all cases). No statistical difference (ns) in P/T ratio was observed between control wing discs and wing discs homozygous mutant for *egr* or *grnd* or expressing *grnd-i* [*O*: *P*(*Ras-V12*, *dlg1-i*) = 0.2743; *P*(*rod-i*, *p35*) = 0.5392]; *P*: *P*(*Ras-V12*, *dlg1-i*) = 0.4149; *P*(rod-i, *p35*) = 0.2906]; *Q*: *P*(*Ras-V12*, *dlg1-i*) = 0.8497; *P*(*rod-i*, *p35*) = 0.92].

mechanistic basis underlying the differential contribution of Grnd to JNK activation in eye and wing primordia is so far little understood. Altogether, these results indicate that JNK activation and growth of CIN and polarity-impaired epithelial tumors can

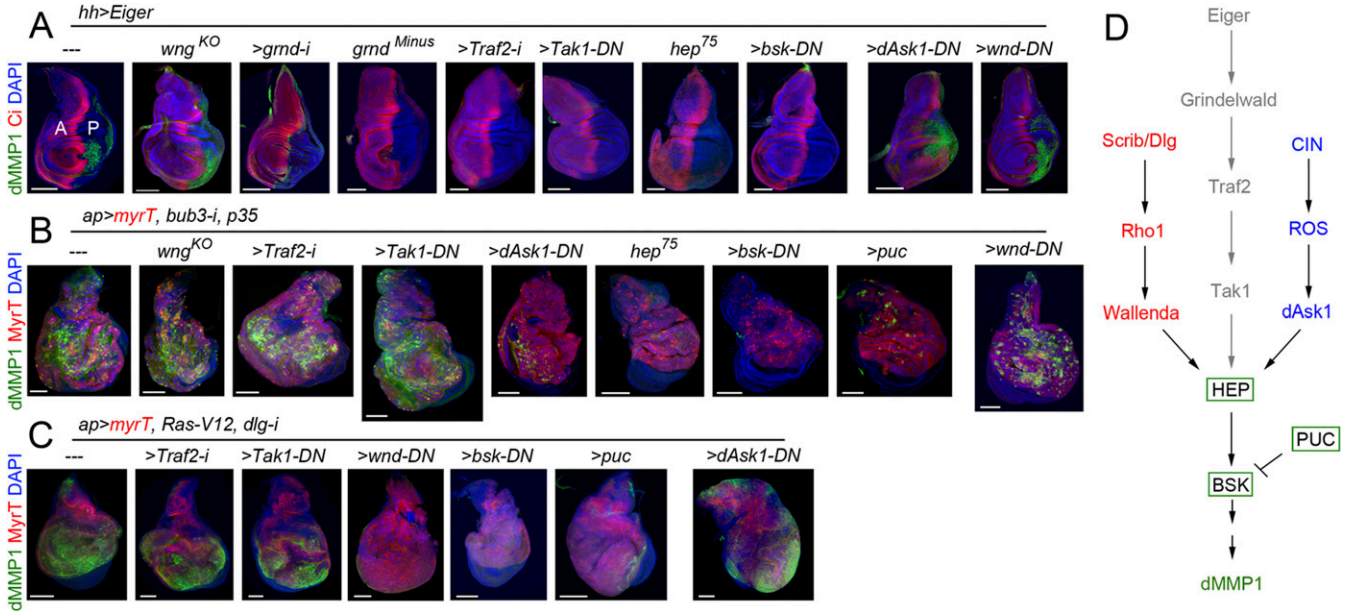

Fig. 7. Multiple Eiger-independent mechanisms to drive JNK activation in epithelial tumors. (*A*–*C*) Larval wing primordia of the indicated genotypes and stained for DAPI (blue), Ci (*A*, red), or MyrT (red, *B* and *C*) and dMMP1 (green). *hh-GAL4* drives expression to posterior (marked as "P") cells, and Ci labels the anterior (marked as "A") compartment. (Scale bars, 100 μm.) (*D*) Cartoon depicting three distinct molecular mechanisms driving JNK activation.

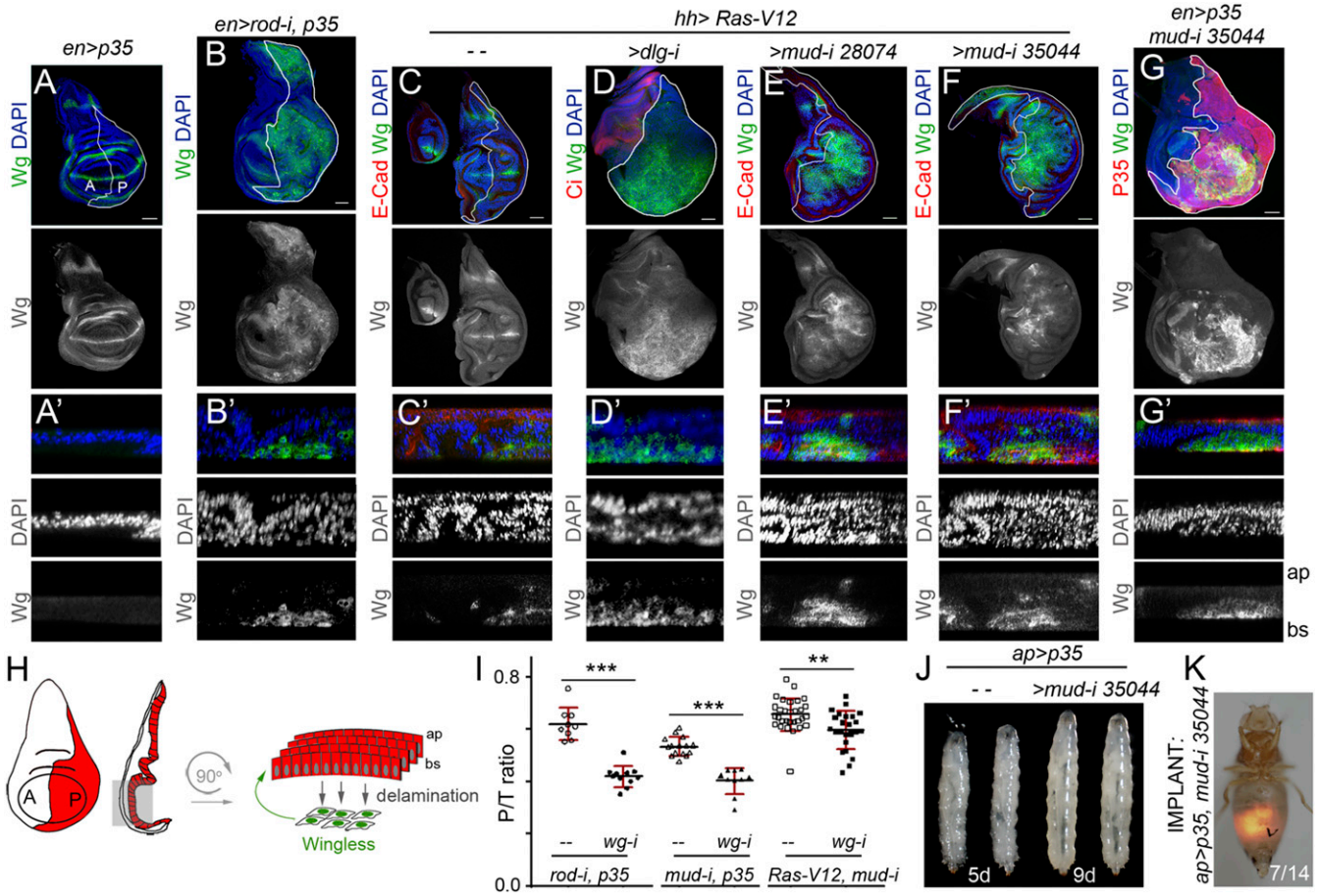

Fig. 8. Wg expression in delaminating cells drives growth in epithelial tumors. (*A*–*G*′) Larval wing primordia of the indicated genotypes and stained for DAPI (blue or white), Wg (green or white), and E-cadherin (E-Cad; red, *C*–*F*′) or P35 (*G*, red). *hh-GAL4* and *en-GAL4* drive expression to posterior (marked as "P") cells (marked by a white line or by the expression of P35). (Scale bars, 50 μm.) In *A*′–*G*′, cross-sections of larval wing primordia are shown to visualize delaminating cells expressing Wg in CIN (*B*′) and polarity-impaired (*D*′) tumor models or upon depletion of *mud* (*E*′, *F*′, and *G*′) compared with wing discs expressing P35 (*A*′) or Ras-V12 (*C*′). Apical (ap) and basal (bs) sides of the epithelium are marked, as are anterior (marked as "A") and posterior (marked as "P") compartments. (*H*) Cartoon depicting a wing disk in which cells in the posterior compartment (red) delaminate basally (bs) and express Wg (green), which drives the proliferation of nondelaminating cells (red). (*I*) Histogram plotting the ratio between the size of the posterior (marked as "P") compartment and the total size (marked as "T") of wing discs of the indicated genotypes. Error bars indicate SD ($n > 9$ in all cases; $^{***}P < 0.001$ and $^{**}P < 0.01$). (*J*) Larvae expressing p35 alone [4 days after egg-laying (AEL)] or in combination with *mud-RNAi* (8 days AEL) under the control of the *ap-GAL4* driver. (*K*) Micrograph of an adult fly carrying a MyrT-labeled (red) implant of the indicated genotype. Image was taken 12 days after implantation; ratio indicates the reproducibility of the phenotype.

happen in the absence of Eiger and Grnd activities, and suggest that JNK activation in these tumors is most probably a cell-autonomous process.

Dissecting the Molecular Mechanisms Underlying JNK Activation. In vertebrate and invertebrate tissues, the conserved JNK pathway integrates signals from a diverse range of stimuli to elicit an appropriate physiological response. Within the *Drosophila* JNK cascade, JNKK/Hemipterous (Hep) phosphorylates JNK/Basket (Bsk) to activate, also by phosphorylation, the AP1 transcriptional complex. Upstream of Hep, different JNKK kinases have been identified in *Drosophila*, including Tak1, Ask1, and Wallenda (Wnd). Tak1 is involved in Eiger/Grnd-mediated JNK activation by binding to Traf2, a member of the TNF receptor-associated factor (TRAF) protein family (14). Consistent with these results, depletion of Grnd or Traf2 by RNAi, or expression of a kinase-dead isoform of Tak1 that acts as a dominant-negative version of the kinase (Tak1-DN) (35), in wing discs overexpressing Eiger rescued JNK activation, monitored by the expression of dMMP1 (Fig. 7*A*). By contrast, depletion of Traf2 or Tak1 activities did not reduce the levels of JNK activation of CIN and polarity-impaired tumors (Fig. 7 *B* and *C*), reinforcing our results unraveling the Eiger/Grnd-independent activation of JNK in these tumors. We observed that loss of Wengen (Wgn), which was identified as the first *Drosophila* TNF receptor (36) and was recently shown to be dispensable for Eiger-induced JNK activation in epithelial cells and RAS-induced tumorigenesis (14), did not rescue JNK activation in CIN tumors either (Fig. 7*B*). CIN tumors bear a large number of aneuploid cells, and the production of radical oxygen species (ROS) in these cells, most probably as a consequence of metabolic stress, contributes to JNK activation (25). A potential JNKK kinase able to phosphorylate Hep and activate Bsk in CIN-induced aneuploid cells is Ask1, as it is directly regulated by ROS through its binding to thioredoxin (37). Whereas the reduced version of thioredoxin binds Ask1 and suppresses its kinase activity, its ROS-induced oxidized version dissociates from Ask1, which becomes active. Interestingly, expression of a kinase-dead mutant form of Ask1, acting as a dominant-negative version of the kinase (Ask1-DN) (38), was able to rescue JNK activation in CIN tumors (Fig. 7*B*). The JNKK kinase Wnd has been identified as an important molecular link that mediates loss of cell polarity-triggered JNK activation (39). Expression of a kinase-dead form of Wnd (Wnd-DN) (40) largely rescued JNK activation in polarity-impaired tumors (Fig. 7*C*). Interestingly, a kinase-dead

version of Bsk (Bsk-DN) (41), a hypomorphic allele of *hep* (*hep*^{75}), or overexpression of Puckered, a phosphatase that inactivates Bsk, were all able to rescue JNK activation in wing discs overexpressing Eiger and in CIN and polarity-impaired tumors (Fig. 7 *A*–*C*) (8, 12, 23), implying that the core Hep/Bsk/Puc module integrates signals from different stimuli. By contrast, the JNKK kinases Tak1, Ask1, and Wnd are the ones sensing context-dependent stimuli, as the capacity of dominant-negative versions of these three kinases to block JNK activation was restricted to Eiger overexpression and CIN and polarity-impaired tumors, respectively (Fig. 7 *A*–*C*). All together, these results reinforce the tissue-autonomous character of JNK activation in CIN and polarity-impaired tumors and unravel different cell-autonomous routes to activate JNK in a tumor-specific manner (Fig. 7*D*).

A Tumor-Intrinsic Mechanism Confers Unlimited Growth Potential. We next characterized the mechanistic basis underlying the TME-independent growth potential of CIN and polarity-impaired tumors and the types of intratumor cell interactions involved. Remarkably, the gene-expression program promoting malignancy as well as the molecular and cellular mechanisms underlying CIN-induced tumor growth resemble those caused by the cooperative action of RAS oncogene activation and mutations in the *scrib* or *dlg1* tumor-suppressor genes (7–10, 12, 25, 26, 42, 43). Loss of cell-polarity determinants or CIN-induced aneuploidy induces cell delamination, and delaminating cells express mitogenic molecules like Wg (the *Drosophila* ortholog of mammalian Wnts) and IL-6–like Upd cytokines, which activate the JAK/STAT pathway (17, 23, 25, 42) (Fig. 8 *A*–*D* and *H* and Fig. S5). These two mitogenic molecules signal back to the tumor mass to drive growth, as depletion of JAK/STAT signaling or Wg reduced tumor growth (17, 23, 25) (Fig. 8*I*). These results highlight the nonautonomous and growth-promoting role of delaminating cells expressing Wg and Upd in CIN and polarity-impaired tumors. We then addressed whether the simple production of delaminating cells expressing mitogenic molecules was sufficient to drive tumor growth. Scrib or Dlg1 cell-polarity determinants have been shown to direct the planar orientation of the mitotic spindle, and failure to orient the mitotic spindle leads to cell delamination and JNK activation (44). Mitotic spindles are oriented by the dynein/dynactin motor complex, whose cortical localization depends on Mud/NUMA. Blocking the death of Mud-depleted misaligned cells by expressing p35 or Ras-V12 was sufficient to drive tumor-like structures formed by Wg- and Upd-expressing delaminating cells located on the basal side of the epithelium and epithelial cells actively proliferating (Fig. 8 *E*–*G* and Fig. S5) (44). Similarly to CIN and polarity-impaired tumors (23, 45, 46), larvae containing *mud*/*p35* tumors were developmentally delayed and became gigantic, and these tumors were malignant to the host and able to grow in allograft transplantations (Fig. 8 *J* and *K* and Fig. S5). Interestingly, depletion of Wg in *mud*-depleted tissues reduced tissue overgrowth (Fig. 8*I*). These results indicate that the simple production of delaminating cells expressing Wg, by means of compromising the planar orientation of the mitotic spindle, is sufficient to promote tumor-like overgrowths. As *scrib*- or *dlg1*-depleted tissues show defects in the planar orientation of the mitotic spindle (44), the observed ectopic expression of Wg in polarity-impaired tumors (Fig. 8*D* and Fig. S5) is also expected to contribute to their growth.

We noticed that mitotic activity in CIN and polarity-impaired tumors was highly increased in the cell population expressing the tumor-initiating transgenes (Fig. 9 *A*–*C*). Interestingly, mitotic activity was restricted to the nondelaminating cell population and absent in Wg-expressing cells (Fig. 9 *D* and *E*), suggesting that the latter cells are mitotically inactive. In CIN tumors, the Wg-dependent resulting hyperproliferation is expected to increase the chances of chromosome segregation errors and aneuploidy levels in the nondelaminating cell layer subject to CIN

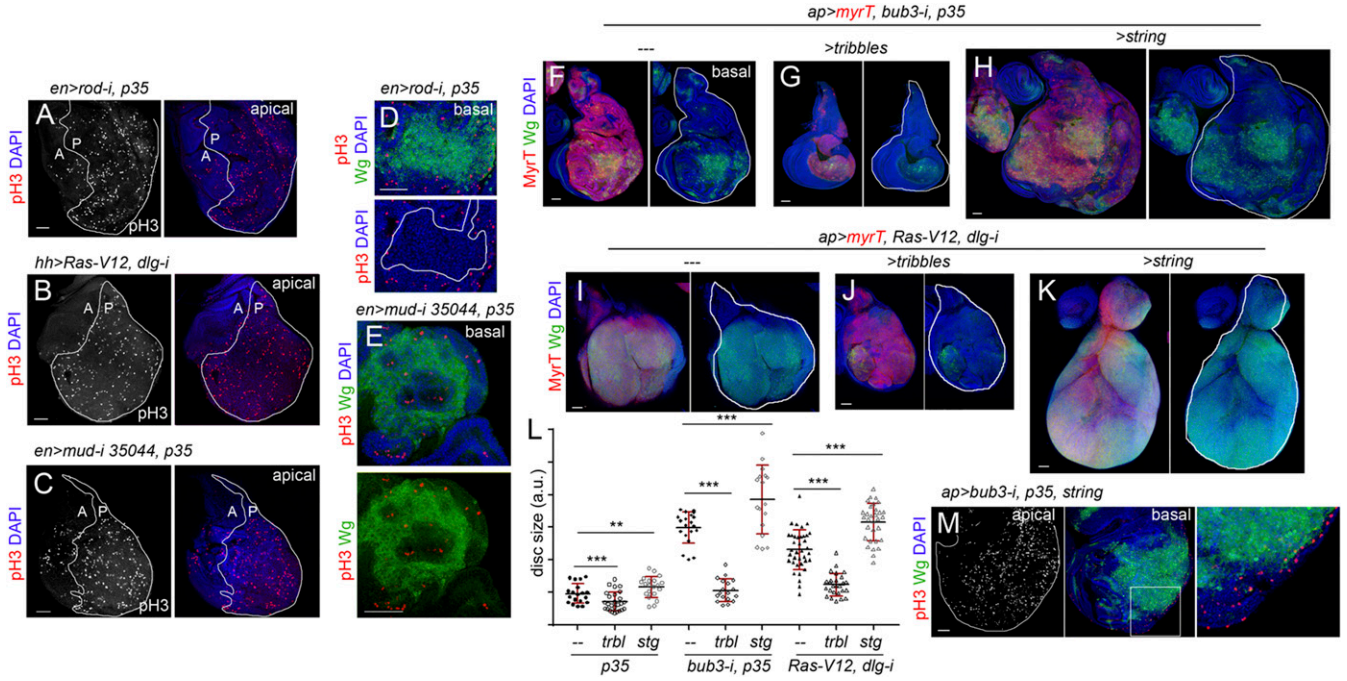

Fig. 9. Mitotic activity increases the number of delaminating cells expressing Wg. (*A*–*K* and *M*) Larval wing primordia of the indicated genotypes and stained for DAPI (blue), pH3 (red or white, *A*–*E* and *M*), Wg (green, *D*–*K*, *M*), and MyrT (red, *F*–*K*). *en-GAL4* drives expression to posterior (marked as "P") cells (marked by a white line in *A*–*C*), and *ap-GAL4* drives expression to dorsal (marked as "D") cells (marked by a white line in *F*–*K* and labeled by the expression of MyrT). Delaminating cells expressing Wg (*D*) or the contour of the disk (*M*) are marked by white lines. (*Right*) Higher magnification of the squared region. (Scale bars, 50 μm.) (*L*) Histogram plotting total size (marked as "T") of wing discs [in arbitrary units (a.u.)] of the indicated genotypes. Error bars indicate SD ($n > 17$ in all cases; $***P < 0.001$ and $**P < 0.01$).

and, consequently, to augment the number of aneuploidy-induced delaminated cells expressing Wg and Upd (47). In polarity-impaired tumors, the augmented cell proliferation in the epithelium, as a response to mitogenic molecules coming from delaminating cells, should also increase the chances of spindle misorientation and cell delamination, and, consequently, the pool of delaminating cells. We tested these proposals by manipulating the proliferating rates in CIN and polarity-impaired tumors and analyzing the impact on the production of Wg-expressing delaminating cells and on the size of the tumors. Overexpression of *Drosophila* Cdc25/String, which drives cells through the G2/M transition (48), or Tribbles, which arrests cells in G2 by ubiquitinating String and sending it to proteasome-mediated degradation (49), do not have a great impact on tissue size in otherwise WT tissues (Fig. 9*L*) (50). By contrast, overexpression of String in CIN and polarity-impaired tumors dramatically increased the number of Wg-expressing cells and tumor size, and Tribbles overexpression reduced the number of Wg-expressing cells and the size of the resulting tumors (Fig. 9 *F*–*K*; quantified in Fig. 9*L*). We noticed that only those cells remaining in the epithelium were mitotically active upon String overexpression (Fig. 9*M*), which is consistent with the proposal that the increase in the number of Wg-expressing cells is a consequence of augmented cell delamination. All together, these results indicate that a feedback amplification loop between delaminating cells expressing mitogenic molecules, which remain mitotically inactive, and the proliferative epithelium acting as source of delaminating cells drives growth and neoplastic transformation of CIN and polarity-impaired tumors in a TME-independent manner. Whether delaminating cells are arrested in G1, as occurs in senescent cells induced in fly epithelial tumors caused by the oncogenic cooperation between Ras-V12 and mitochondrial mutants (51, 52), is an interesting idea that needs to be elucidated but that could certainly explain their resistance to String overexpression.

Discussion

Tumor progression and metastatic colonization at distant sites rely on interactions with the surrounding TME (2, 53). The TME acts as a niche to provide secreted signaling molecules and growth factors that maintain the undifferentiated state of the tumor and promote its growth. Here we used two well-characterized and molecularly distinct JNK-driven epithelial tumors of *Drosophila*, the CIN and polarity-impaired models (23, 26), to unravel TME-independent mechanisms that contribute to the unlimited growth potential of these tumors. We used the *GAL4/UAS* system to drive tumorigenesis in large territories, thus reducing the amount of cell interactions with WT epithelial cells. We combined allograft transplantation experiments with the *GAL4/UAS* and *lexA/lexO* transactivation systems to ablate TME cells and analyzed the impact on tumor initiation and JNK activation. We present evidence that genetic ablation of resident myoblasts or recruited hemocytes, by means of expression of the proapoptotic gene *reaper*, does not prevent tumor formation or JNK activation in CIN or polarity-impaired models. Our results support the notion that, in the absence of a TME, the growth potential of these tumors is determined by interactions between functionally distinct cell populations within the tumors (Fig. 10*A*). It is interesting to note in this context that the two interacting cell populations within CIN tumors are clearly genetically distinct, as delaminating cells are highly aneuploid, whereas these two cell populations are genetically similar in RAS tumors. Cancer has been classically understood as a cell-autonomous process by which oncogenes and loss of tumor-suppressor genes drive clonal cell expansion. However, research in a variety of model organisms, including *Drosophila*, has unveiled the relevance of cell communication in tumor development (reviewed in refs. 3, 4). Interactions between tumor cells and the surrounding TME, and between clonally distinct cell populations, have been shown to contribute to tumor progression and metastatic colonization. Our work supports the notion that intratumor communication also between genetically similar but functionally distinct cell populations can contribute to tumor growth. Remarkably, in all these relevant social interactions, secreted signaling molecules and growth factors play a similar role in driving proliferation and growth of tumor cells.

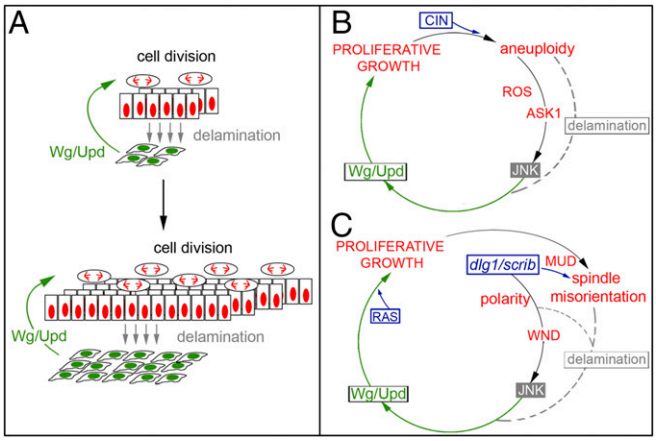

Fig. 10. A feedback amplification loop drives unlimited growth in epithelial tumors. (*A*) Cartoon depicting the cell populations and interactions responsible to the unlimited growth potential of epithelial tumors. While Wg and Upd emanating from basally delaminating cells (in green) promotes proliferative growth of the main epithelium (in red), the resulting increase in the number of mitotic events has a positive impact in the number of cells delaminating as a consequence of mistakes in the segregation of chromosomes or planar orientation of the mitotic spindle. (*B*) In CIN tumors, aneuploid cells activate in an ROS- and Ask1-dependent manner, JNK, which induces the expression of Wg and Upd. Those cells with the highest levels of aneuploidy delaminate basally and drive, through Wg and Upd, the proliferation of nondelaminating cells. Cell proliferation increases the chances of chromosome segregation errors and the levels of aneuploidy and, consequently, the pool of aneuploidy-induced delaminating cells. (*C*) In polarity-impaired tumors, loss of cell polarity determinants Scrib or Dlg1 activate, in a Wnd-dependent manner, JNK, which induces the expression of Wg and Upd. Defects in apicobasal polarity and planar orientation of the mitotic spindle as a consequence of loss of Scrib or Dlg1 induce cell delamination. Delaminating cells drive, through Wg and Upd, the proliferation of nondelaminating cells. Cell proliferation driven by the combined activities of Wg, Upd, and Ras increases the chances of defects in the planar orientation of the mitotic spindle and, consequently, augments the pool of Wg- and Upd-expressing delaminating cells.

Interactions between tumor cells and the surrounding TME, and between clonally distinct cell populations, have been shown to be mediated by the TNF-α ligand Eiger and its receptor Grnd, which drive JNK activation, tumor growth, and invasive behavior (13–15). However, the conserved JNK pathway can also integrate signals from a diverse range of stimuli to elicit an appropriate physiological response in vertebrate and invertebrate tissues. Here we used CIN and polarity-impaired tumor models in which cell interactions with WT cells are being reduced to present evidence that different routes, sensing cell-autonomous stimuli, are used in a tumor-specific manner to activate a common JNKK/JNK core that induces a shared tumorigenic transcriptional program (Fig. 10 *B* and *C*). CIN tumors induce a large number of aneuploid cells, and the production of ROS in these cells contributes to JNK activation (25). We identified Ask1, which was shown to be directly regulated by ROS through its binding to thioredoxin (37), as the JNKK kinase driving JNK activation in CIN tumors. We present evidence that the JNKK kinase Wnd, which is activated by loss of cell polarity determinants (39), drives JNK activation in polarity-impaired tumors. These results, together with our experimental data ruling out any role of Eiger and Grnd in JNK activation, support the cell-autonomous

character of JNK activation in our CIN and polarity-impaired epithelial tumors and the TME-independent self-reinforcement mechanism that drives their unlimited growth potential.

Materials and Methods

Drosophila strains were obtained from Vienna *Drosophila* RNAi Center or the Bloomington Stock Center and are described in FlyBase. Antibodies were obtained from the Developmental Studies Hybridoma Bank or other private sources. These and other experimental details are described in *SI Materials and Methods*.

ACKNOWLEDGMENTS. We thank I. Ando, K. Basler, J. Colombani, H. Herranz, H. Jiang, P. Leopold, M. Leptin, M. Miura, and F. Serras; the Bloomington *Drosophila* Stock Center, the Vienna *Drosophila* RNAi Center, and the National Institute of Genetics (Japan) for flies; the Developmental Studies Hybridoma Bank for antibodies; and M. Clemente and other members of the laboratory for comments on the manuscript. This work was funded by a PhD fellowship from La Caixa (to L.M.), Ministerio de Economía, Industria y Competitividad (MINECO) (Government of Spain) Grants SIGNAGROWTH-BFU2013-44485 and INTERGROWTH-BFU2016-77587-P (to M. Milán), and Fondo Europeo de Desarrollo Regional (FEDER) "Una manera de hacer Europa" (M. Milán). Institute for Research in Biomedicine (IRB Barcelona) is the recipient of a Severo Ochoa Award of Excellence from MINECO. M. Milán is an Institució Catalana de Recerca i Estudis Avançats (ICREA) Research Professor.

1. Hanahan D, Weinberg RA (2011) Hallmarks of cancer: The next generation. *Cell* 144: 646–674.
2. Quail DF, Joyce JA (2013) Microenvironmental regulation of tumor progression and metastasis. *Nat Med* 19:1423–1437.
3. Tabassum DP, Polyak K (2015) Tumorigenesis: It takes a village. *Nat Rev Cancer* 15: 473–483.
4. Pastor-Pareja JC, Xu T (2013) Dissecting social cell biology and tumors using Drosophila genetics. *Annu Rev Genet* 47:51–74.
5. Cordero JB, et al. (2010) Oncogenic Ras diverts a host TNF tumor suppressor activity into tumor promoter. *Dev Cell* 18:999–1011.
6. Uhlirova M, Jasper H, Bohmann D (2005) Non-cell-autonomous induction of tissue overgrowth by JNK/Ras cooperation in a Drosophila tumor model. *Proc Natl Acad Sci USA* 102:13123–13128.
7. Brumby AM, Richardson HE (2003) scribble mutants cooperate with oncogenic Ras or Notch to cause neoplastic overgrowth in Drosophila. *EMBO J* 22:5769–5779.
8. Igaki T, Pagliarini RA, Xu T (2006) Loss of cell polarity drives tumor growth and invasion through JNK activation in Drosophila. *Curr Biol* 16:1139–1146.
9. Figueroa-Clarevega A, Bilder D (2015) Malignant Drosophila tumors interrupt insulin signaling to induce cachexia-like wasting. *Dev Cell* 33:47–55.
10. Külshammer E, et al. (2015) Interplay among Drosophila transcription factors Ets21c, Fos and Ftz-F1 drives JNK-mediated tumor malignancy. *Dis Model Mech* 8:1279–1293.
11. Külshammer E, Uhlirova M (2013) The actin cross-linker Filamin/Cheerio mediates tumor malignancy downstream of JNK signaling. *J Cell Sci* 126:927–938.
12. Uhlirova M, Bohmann D (2006) JNK- and Fos-regulated Mmp1 expression cooperates with Ras to induce invasive tumors in Drosophila. *EMBO J* 25:5294–5304.
13. Igaki T, Pastor-Pareja JC, Aonuma H, Miura M, Xu T (2009) Intrinsic tumor suppression and epithelial maintenance by endocytic activation of Eiger/TNF signaling in Drosophila. *Dev Cell* 16:458–465.
14. Andersen DS, et al. (2015) The Drosophila TNF receptor Grindelwald couples loss of cell polarity and neoplastic growth. *Nature* 522:482–486.
15. Ohsawa S, et al. (2011) Elimination of oncogenic neighbors by JNK-mediated engulfment in Drosophila. *Dev Cell* 20:315–328.
16. Katheder NS, et al. (2017) Microenvironmental autophagy promotes tumour growth. *Nature* 541:417–420.
17. Wu M, Pastor-Pareja JC, Xu T (2010) Interaction between Ras(V12) and scribbled clones induces tumour growth and invasion. *Nature* 463:545–548.
18. Pastor-Pareja JC, Wu M, Xu T (2008) An innate immune response of blood cells to tumors and tissue damage in Drosophila. *Dis Model Mech* 1:144–154, discussion 153.
19. Herranz H, Weng R, Cohen SM (2014) Crosstalk between epithelial and mesenchymal tissues in tumorigenesis and imaginal disc development. *Curr Biol* 24:1476–1484.
20. Moreno E, Yan M, Basler K (2002) Evolution of TNF signaling mechanisms: JNK-dependent apoptosis triggered by Eiger, the Drosophila homolog of the TNF superfamily. *Curr Biol* 12:1263–1268.
21. Igaki T, et al. (2002) Eiger, a TNF superfamily ligand that triggers the Drosophila JNK pathway. *EMBO J* 21:3009–3018.
22. Schvartzman JM, Sotillo R, Benezra R (2010) Mitotic chromosomal instability and cancer: Mouse modelling of the human disease. *Nat Rev Cancer* 10:102–115.
23. Dekanty A, Barrio L, Muzzopappa M, Auer H, Milán M (2012) Aneuploidy-induced delaminating cells drive tumorigenesis in Drosophila epithelia. *Proc Natl Acad Sci USA* 109:20549–20554.
24. Hay BA, Wolff T, Rubin GM (1994) Expression of baculovirus P35 prevents cell death in Drosophila. *Development* 120:2121–2129.
25. Clemente-Ruiz M, et al. (2016) Gene dosage imbalance contributes to chromosomal instability-induced tumorigenesis. *Dev Cell* 36:290–302.
26. Pagliarini RA, Xu T (2003) A genetic screen in Drosophila for metastatic behavior. *Science* 302:1227–1231.
27. Humbert PO, et al. (2008) Control of tumourigenesis by the Scribble/Dlg/Lgl polarity module. *Oncogene* 27:6888–6907.
28. Dow LE, et al. (2008) Loss of human Scribble cooperates with H-Ras to promote cell invasion through deregulation of MAPK signalling. *Oncogene* 27:5988–6001.
29. Dow LE, et al. (2003) hScrib is a functional homologue of the Drosophila tumour suppressor Scribble. *Oncogene* 22:9225–9230.
30. Prober DA, Edgar BA (2000) Ras1 promotes cellular growth in the Drosophila wing. *Cell* 100:435–446.
31. Blochlinger K, Jan LY, Jan YN (1993) Postembryonic patterns of expression of *cut*, a locus regulating sensory organ identity in *Drosophila*. *Development* 117:441–450.
32. Kurucz E, et al. (2007) Nimrod, a putative phagocytosis receptor with EGF repeats in Drosophila plasmatocytes. *Curr Biol* 17:649–654.
33. Kurucz E, et al. (2003) Hemese, a hemocyte-specific transmembrane protein, affects the cellular immune response in Drosophila. *Proc Natl Acad Sci USA* 100:2622–2627.
34. McGuire SE, Mao Z, Davis RL (2004) Spatiotemporal gene expression targeting with the TARGET and gene-switch systems in Drosophila. *Sci STKE* 2004:pl6.
35. Mihaly J, et al. (2001) The role of the Drosophila TAK homologue dTAK during development. *Mech Dev* 102:67–79.
36. Kanda H, Igaki T, Kanuka H, Yagi T, Miura M (2002) Wengen, a member of the Drosophila tumor necrosis factor receptor superfamily, is required for Eiger signaling. *J Biol Chem* 277:28372–28375.
37. Sekine Y, et al. (2012) The Kelch repeat protein KLHDC10 regulates oxidative stress-induced ASK1 activation by suppressing PP5. *Mol Cell* 48:692–704.
38. Kuranaga E, et al. (2002) Reaper-mediated inhibition of DIAP1-induced DTRAF1 degradation results in activation of JNK in Drosophila. *Nat Cell Biol* 4: 705–710.
39. Ma X, et al. (2016) Rho1-Wnd signaling regulates loss-of-cell polarity-induced cell invasion in Drosophila. *Oncogene* 35:846–855.
40. Collins CA, Wairkar YP, Johnson SL, DiAntonio A (2006) Highwire restrains synaptic growth by attenuating a MAP kinase signal. *Neuron* 51:57–69.
41. Weber U, Paricio N, Mlodzik M (2000) Jun mediates Frizzled-induced R3/R4 cell fate distinction and planar polarity determination in the Drosophila eye. *Development* 127:3619–3629.
42. Bunker BD, Nellimoottil TT, Boileau RM, Classen AK, Bilder D (2015) The transcriptional response to tumorigenic polarity loss in Drosophila. *eLife* 4:4.
43. Atkins M, et al. (2016) An ectopic network of transcription factors regulated by Hippo signaling drives growth and invasion of a malignant tumor model. *Curr Biol* 26: 2101–2113.
44. Nakajima Y, Meyer EJ, Kroesen A, McKinney SA, Gibson MC (2013) Epithelial junctions maintain tissue architecture by directing planar spindle orientation. *Nature* 500: 359–362.
45. Garelli A, Gontijo AM, Miguela V, Caparros E, Dominguez M (2012) Imaginal discs secrete insulin-like peptide 8 to mediate plasticity of growth and maturation. *Science* 336:579–582.
46. Colombani J, Andersen DS, Léopold P (2012) Secreted peptide Dilp8 coordinates Drosophila tissue growth with developmental timing. *Science* 336:582–585.
47. Milán M, Clemente-Ruiz M, Dekanty A, Muzzopappa M (2014) Aneuploidy and tumorigenesis in Drosophila. *Semin Cell Dev Biol* 28:110–115.
48. Edgar BA, O'Farrell PH (1990) The three postblastoderm cell cycles of Drosophila embryogenesis are regulated in G2 by string. *Cell* 62:469–480.
49. Mata J, Curado S, Ephrussi A, Rørth P (2000) Tribbles coordinates mitosis and morphogenesis in Drosophila by regulating string/CDC25 proteolysis. *Cell* 101:511–522.
50. Neufeld TP, de la Cruz AF, Johnston LA, Edgar BA (1998) Coordination of growth and cell division in the Drosophila wing. *Cell* 93:1183–1193.
51. Ohsawa S, et al. (2012) Mitochondrial defect drives non-autonomous tumour progression through Hippo signalling in Drosophila. *Nature* 490:547–551.
52. Nakamura M, Ohsawa S, Igaki T (2014) Mitochondrial defects trigger proliferation of neighbouring cells via a senescence-associated secretory phenotype in Drosophila. *Nat Commun* 5:5264.
53. Joyce JA, Pollard JW (2009) Microenvironmental regulation of metastasis. *Nat Rev Cancer* 9:239–252.
54. Evans CJ, et al. (2009) G-TRACE: Rapid Gal4-based cell lineage analysis in Drosophila. *Nat Methods* 6:603–605.
55. Bergmann A, Agapite J, McCall K, Steller H (1998) The Drosophila gene hid is a direct molecular target of Ras-dependent survival signaling. *Cell* 95:331–341.
56. Doggett K, Grusche FA, Richardson HE, Brumby AM (2011) Loss of the Drosophila cell polarity regulator Scribbled promotes epithelial tissue overgrowth and cooperation with oncogenic Ras-Raf through impaired Hippo pathway signaling. *BMC Dev Biol* 11: 57.
57. Zhang Y, You J, Ren W, Lin X (2013) Drosophila glypicans Dally and Dally-like are essential regulators for JAK/STAT signaling and Unpaired distribution in eye development. *Dev Biol* 375:23–32.
58. Martín-Blanco E, et al. (1998) puckered encodes a phosphatase that mediates a feedback loop regulating JNK activity during dorsal closure in Drosophila. *Genes Dev* 12:557–570.
59. Yagi R, Mayer F, Basler K (2010) Refined LexA transactivators and their use in combination with the Drosophila Gal4 system. *Proc Natl Acad Sci USA* 107:16166–16171.
60. Jiang H, Grenley MO, Bravo MJ, Blumhagen RZ, Edgar BA (2011) EGFR/Ras/MAPK signaling mediates adult midgut epithelial homeostasis and regeneration in Drosophila. *Cell Stem Cell* 8:84–95.
61. Leptin M (1991) twist and snail as positive and negative regulators during Drosophila mesoderm development. *Genes Dev* 5:1568–1576.
62. Ursprung H (1967) *In Vivo Culture of Drosophila Imaginal Discs* (T.Y. Crowell, New York), pp 485–492.